Stability of the car-following model on two lanes

Tie-Qiao Tang,[1] Hai-Jun Huang,[1,*] and Zi-You Gao[2]
[1]*School of Management, Beijing University of Aeronautics and Astronautics, Beijing 100083, China*
[2]*School of Traffic and Transportation, Beijing Jiaotong University, Beijing 100044, China*
(Received 16 April 2005; published 23 December 2005)

In the case of two-lane traffic, vehicle drivers always worry about the lane changing actions from neighbor lane. This paper studies the stability of a car-following model on two lanes which incorporates the lateral effects in traffic. The stability condition of the model is obtained by using the linear stability theory. The modified Korteweg–de Vries equation is constructed and solved, and three types of traffic flows in the headway-sensitivity space—stable, metastable, and unstable—are classified. Both analytical and simulation results show that the anxiousness about lane changing from neighbor lane indeed has influence upon people's driving behavior and the consideration of lateral effects could stabilize the traffic flows on both lanes.

DOI: 10.1103/PhysRevE.72.066124 PACS number(s): 05.70.Fh, 05.70.Jk

I. INTRODUCTION

An increasing number of traffic models have been developed and empirically tested (see the review paper by Chowdhury *et al.* [1]). In 1995, Bando *et al.* [2] proposed an optimal velocity (OV) model for characterizing the car-following behavior, and then extended it with the consideration of explicit delay time [3]. Davis [4] found that keeping safe platoons only requires short delay times which are remarkably smaller than the typical reaction times of driving. Recently, Lubashevsky *et al.* [5] further extended the work [3] through introducing the deficiencies of human decision making in driving. The OV model can be used to analyze various traffic density waves when combined with perturbation method. Using this model, Komatsu and Sasa [6] derived the modified Korteweg–de Vries (MKDV) equation and described traffic jam as a kink density wave. Nagatani *et al.* [7] took the effect of acceleration delay into account in the OV model and obtained Korteweg–de Vries (KDV) equation from the nonlinear analysis near the critical point. Muramatsu and Nagatani [8] showed that the solitonary density wave appears near the neutral stability line only. Nagatani [9] also extended the OV model by considering the vehicle interaction with the next car ahead (i.e., the next-nearest-neighbor interaction) and showed that the triangular shock wave, soliton wave and kink wave appear in three regions (i.e., stable, metastable, and unstable) given by the solutions of Burgers equation, KDV equation, and MKDV equation, respectively.

In 1998, Helbing and Tilch [10] carried out a calibration of the OV model using the empirical follow-the-leader data and found that an extremely short relaxation time could result in a very high value of acceleration that led to an overshooting of the vehicle velocity. They then developed a generalized force (GF) model. The GF model can overcome some deficiencies of the OV model, but both these two models can not capture such behavior that the following vehicle may not decelerate if the preceding vehicle travel faster than itself although the distance between them is shorter than the safe distance for an instant [11]. Lubashevsky *et al.* [12] reported that Helly [13] did a similar approximation in the year as early as 1959. Later, Treiber *et al.* [14,15] developed an intelligent driver model that forms a collision-free description of car one-lane ensembles. On the other hand, Jiang *et al.* [16,17] proposed a full velocity difference model which considers more aspects in car-following process than the OV and GF models and theoretically is more realistic.

Recently, Xue *et al.* [18–20] presented a simplified OV model for investigating the effects of the relative velocity. They derived the MKDV equation for describing the traffic jam in unstable region, obtained the phase diagram $(\Delta x, \alpha)$ (Δx is the headway and α the sensitivity coefficient) under various values of the response factor to relative velocity, and divided the traffic flow into stable, metastable and unstable regions [18,20]. Xue [21] proposed a lattice model of optimized traffic flow with the consideration of optimal current with the next-nearest-neighbor interaction. Lenz *et al.* [22] constructed a model that a driver looks at many vehicles ahead of him/her. Hasebe *et al.* [23,24] presented an extended OV model applied to a cooperative driving control system. They found that there exist a certain set of parameters that make traffic flow "most stable" in their "forward looking" OV model. Ge *et al.* [25] showed that a drive does not necessarily consider the effects from an arbitrary number of vehicles ahead of him/her but that from the three vehicles ahead of him/her. But the dynamic behaviors near the critical points of the model parameters have not been investigated in these studies. Orosz *et al.* [26] investigated the local and global bifurcations of OV model with driver reaction time and numerically found several regions of multistability.

The list of contributions associated with the OV model is still becoming larger. However, all existing models are only subject to singe lane traffic. In this paper, we first present an extended car-following model on two lanes by incorporating the lateral effects in traffic. We then derive the models' stability condition by using the linear stability theory. Three types of traffic flows, namely, stable, metastable, and un-

*Email address: hjhuang@mail.nsfc.gov.cn

stable ones, are classified by analyzing the neutral stability curves and the coexisting curves given by the solution of the MKDV equation. Numerical simulation is carried out to validate the analytic results. We find that our model is superior in stability to other models due to the consideration of lateral effects. This implies that the lateral effects could make traffic flow more stable.

II. MODEL

The dynamic equation of the car-following model on single-lane highway takes in general the following form [1]:

$$x_n'' = f_{\mathrm{sti}}(v_n, \Delta x_n, \Delta v_n), \tag{1}$$

where the function f_{sti} represents the response received by the nth vehicle to stimulus. Equation (1) defines the acceleration or deceleration of the nth vehicle, which is determined by the surrounding traffic conditions. The stimulus is composed of the velocity v_n, the velocity difference $\Delta v_n = v_{n+1} - v_n$, and the headway $\Delta x_n = x_{n+1} - x_n$ between successive vehicles. A representative dynamic equation of car-following models is as follows [16–20]:

$$\frac{dx_n(t+\tau)}{dt} = V(\Delta x_n(t), \Delta v_n(t)), \tag{2}$$

where $x_n(t)$ is the position of the nth vehicle at time t, $V(\Delta x_n(t), \Delta v_n(t))$ is the optimal velocity formulated as a function of the headway and relative velocity, and τ denotes the delay time with which the vehicle velocity reaches the optimal velocity as the traffic flow is varying.

In the case of two-lane traffic, besides the effects in front, the lateral effects should also be taken into account. This is because our survey made in Beijing shows that the driving behavior of a vehicle on a lane is somewhat influenced by the traffic flow on neighbor lane. Few drivers suddenly change lanes without any alert message to neighbor lane cars, with the result that most drivers have to be ready to take precautions against the nearest vehicle on neighbor lane in front of him/her lane at any moment (although the lane changing actions do not occur). This may be unique in comparison with other countries since the driving behavior has not been regulated perfectly yet in the rapidly developing China. Hence, Eq. (1) should be adjusted as follows:

$$x_{l,n_l}'' = f_{\mathrm{sti}}^{l}(v_{l,n_l}, \Delta x_{l,n_l}, \Delta_{l,n_l}, \Delta v_{l,n_l}), \tag{3}$$

where l represent the lane number ($l=1,2$), Δ_{l,n_l} is the distance between the n_lth vehicle on lane l and the nearest vehicle on neighbor lane in front of this vehicle. Note that the lateral velocity difference is not considered in this paper. Then, the car-following model Eq. (2) becomes

$$\frac{dx_{l,n_l}(t+\tau_l)}{dt} = V_l(\Delta x_{l,n_l}(t), \Delta_{l,n_l}(t), \Delta v_{l,n_l}(t)). \tag{4}$$

Expanding the left hand side of Eq. (4) in Taylor series with small parameter τ_l and omitting the high order terms, we have $dx_{l,n_l}(t+\tau_l)/dt = dx_{l,n_l}(t)/dt + \tau_l d^2 x_{l,n_l}(t)/dt^2$. Let the optimal velocity be a linear combination of the headway-expressed velocity and the current velocity difference, i.e., $V_l(\Delta x_{l,n_l}(t), \Delta_l(t), \Delta v_{l,n_l}(t)) = V_l(\Delta x_{l,n_l}(t), \Delta_{l,n_l}(t)) + \lambda_l \Delta v_{l,n_l}(t)$, where the response factor to relative velocity, λ_l ($0 \leqslant \lambda_l \leqslant 1$), is a constant independent of time, velocity and position, and $\lambda_1 > \lambda_2$ holds since the physical condition for driving on lane 1 is assumed to be better than lane 2 in our study. Therefore, Eq. (4) can be rewritten as

$$\frac{d^2 x_{l,n_l}(t)}{dt^2} = \alpha_l \left(V_l(\Delta x_{l,n_l}(t), \Delta_{l,n_l}(t)) - \frac{dx_{l,n_l}}{dt} \right) + \kappa_l \Delta v_{l,n_l}(t), \tag{5}$$

where $\alpha_l = 1/\tau_l$ represents the sensitivity coefficient of a driver on lane l to the difference between the optimal and the current velocities, and $\kappa_l = \lambda_l/\tau_l$ is the sensitivity coefficient of response to the stimulus $\Delta v_{l,n_l}(t)$.

Up to now, we have motivated a time continuous car-following model for highway with two lanes. To perform the model's stability analyses, we have to further discretize it. By using the asymmetric forward difference, we rewrite Eq. (5) as follows:

$$\begin{aligned} x_{l,n_l}(t+2\tau_l) = {} & x_{l,n_l}(t+\tau_l) + \tau_l V_l(\Delta x_{l,n_l}(t), \Delta_{l,n_l}(t)) \\ & + \lambda_l \tau_l [\Delta x_{l,n_l}(t+\tau_l) - \Delta x_{l,n_l}(t)]. \end{aligned} \tag{6}$$

Define a weighted headway $\Delta \bar{x}_{l,n_l} = \beta_1 \Delta x_{l,n_l} + \beta_2 \Delta_{l,n_l}$, where β_1 and β_2 are the weights of axial headway $\Delta x_{l,n_l}$ and lateral distance Δ_{l,n_l}, respectively, $\beta_1 + \beta_2 = 1$. The headway-expressed optimal velocity in Eq. (6) is selected similar to that used by Bando *et al.* [2],

$$\begin{aligned} & V_l(\Delta x_{l,n_l}(t), \Delta_{l,n_l}) \\ & \quad = V_l(\Delta \bar{x}_{l,n_l}) = 0.5 v_{\max}^{l} [\tanh(\Delta \bar{x}_{l,n_l} - h_{lc}) + \tanh(h_{lc})], \end{aligned} \tag{7}$$

where h_{lc} is a comprehensive safety parameter reflecting both the axial and lateral effects. This parameter should be larger than the safety distance without lateral effects considered. In our simulation, set $v_{\max}^{1} = 2.5$ m/s, $v_{\max}^{2} = 2$ m/s, $h_{1c} = 4.5$ m and $h_{2c} = 4$ m. The optimal velocity Eq. (7) is a monotonically increasing function of the weighted distance and is bounded by the maximal velocity $v_{\max}^{l}$. It is clear that when the weighted headway is less than the comprehensive safety parameter, the vehicle velocity is reduced to prevent crashing into the preceding vehicles on both lanes; if it is larger than the parameter, the vehicle velocity increases to the maximum velocity.

The headway-expressed optimal velocity Eq. (7) has a turning point at $\Delta \bar{x}_{l,n_l} = h_{lc}$, where

$$V_l''(\Delta \bar{x}_{l,n_l}) = \left. \frac{d^2 V_l(\Delta \bar{x}_{l,n_l})}{d \Delta \bar{x}_{l,n_l}^2} \right|_{\Delta \bar{x}_{l,n_l} = h_{lc}} = 0. \tag{8}$$

As explained in Ge *et al.* [25], the reason of choosing the form of Bando *et al.* [2] for optimal velocity lies in the existence of the above turning point, which is important for us to derive the MKDV equation from Eq. (6).

III. LINEAR STABILITY ANALYSIS

The method of linear stability analysis similar to Ge *et al.* [25] is applied to the above model. Because there is no real lane changing in our modeling and we only assume there are different numbers of vehicles on both lanes, so the steady state solutions exist for both lanes and their stability analyses can be carried out separately. However, there is a coupling between lane 1 and 2 in examining the lateral effect, we hence adopt the mean-field approach to treat the car ensemble on one lane in some averaged way when the dynamics of cars on the other lane is analyzed. Now, we first consider the stability of a uniform traffic flow on each lane. The uniform traffic flow is defined by such a state that all vehicles on lane l ($l=1,2$) move with the optimal velocity $V_l(h_l,\Delta_l)$ and the identical headway h_l and the lateral distance Δ_l, while the relative velocity $\Delta v_{l,n_l}$ is set to be zero. Clearly, we have

$$x_{l,n_l,0}(t) = h_l n_l + V_l(h_l,\Delta_l)t \quad \text{with } h_l = D/N_l \text{ and } \Delta_l = D/(N_1+N_2), \tag{9}$$

where N_l is the total number of vehicles on lane l, D is the road length, and $x_{l,n_l,0}(t)$ is the position of the n_lth vehicle in steady state.

Let $y_{l,n_l}(t)$ be a small deviation from the steady-state solution $x_{l,n_l,0}(t)$, i.e.,

$$x_{l,n_l}(t) = x_{l,n_l,0}(t) + y_{l,n_l}(t). \tag{10}$$

Substituting Eq. (10) into Eq. (6) and linearizing the resulting equation yield

$$\begin{aligned} y_{l,n_l}(t+2\tau_l) = {} & y_{l,n_l}(t+\tau_l) + \tau_l V_l'(h_l)[\beta_1(y_{l,n_l+1}(t) - y_{l,n_l}(t)) \\ & + \beta_2(\Delta_{l,n_l+1}(t) - \Delta\Delta_{l,n_l}(t))] \\ & + \lambda_l\tau_l[\Delta y_{l,n_l}(t+\tau_l) - \Delta y_{l,n_l}], \end{aligned} \tag{11}$$

where $V_l'(h_l) = dV_l(\Delta\bar{x}_l)/d\Delta\bar{x}_l$ at $\Delta\bar{x}_l = h_l$, and $\Delta\Delta_{l,n_l}(t) = \Delta_{l,n_l+1}(t) - \Delta_{l,n_l}(t)$. For a very small perturbation $y_{l,n_l}(t)$ at $x_{l,n_l,0}(t)$, we can let $\Delta\Delta_{l,n_l}(t) \cong 0.5[\Delta y_{l,n_l+2}(t) - \Delta y_{l,n_l+1}(t)]$. Expanding y_{l,n_l} in the Fourier-modes, i.e., $y_{l,n_l}(t) = A_l \exp(ik_l n_l + z_l t)$, we obtain

$$\begin{aligned} & (e^{z_l\tau_l} - 1)(e^{z_l\tau_l} - \lambda_l\tau_l e^{ik_l} + \lambda_l\tau_l) \\ & \quad = \tau_l V_l'(h_l)[\beta_1(e^{ik_l} - 1) + 0.5\beta_2(e^{2ik_l} - e^{ik_l})]. \end{aligned} \tag{12}$$

Expanding z_l, i.e., $z_l = z_{1l}(ik_l) + z_{2l}(ik_l)^2 +$, and inserting it into the above equation, we obtain the first- and second-order terms of coefficients in the expression of z_l, as follows:

$$z_{1l} = V_l'(h_l)$$
$$\text{and } z_{2l} = -\frac{3V_l'(h_l)\tau_l}{2} + \frac{V_l'(h_l)}{2}(\beta_1 + 1.5\beta_2) + \lambda_l V_l'(h_l), \tag{13}$$

where $l=1,2$.

Thus the neutral stability condition is given by

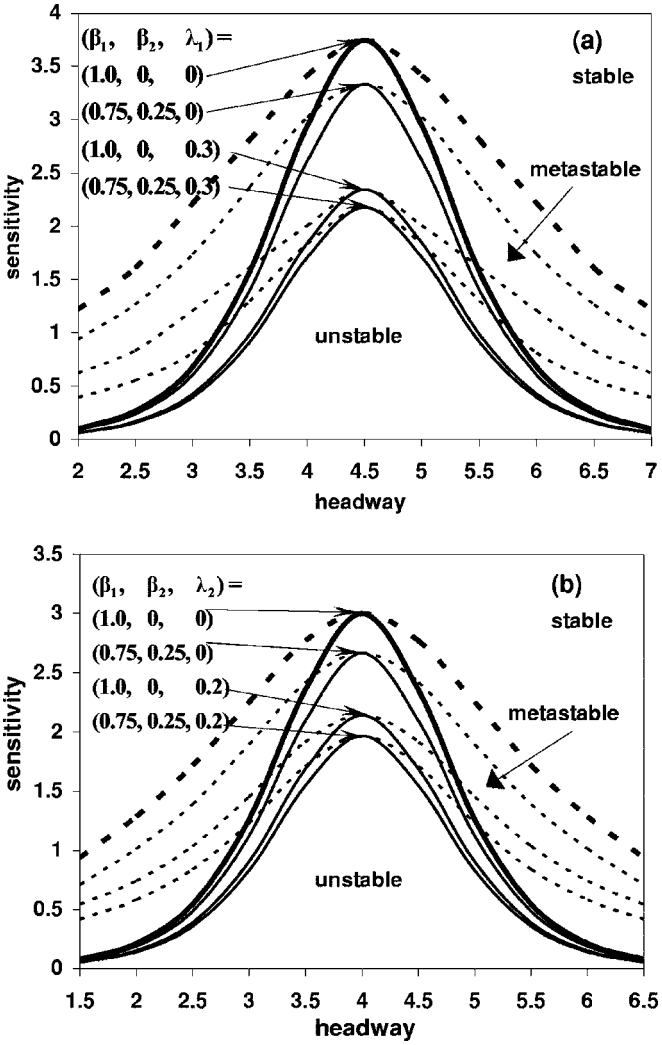

FIG. 1. Phase diagram in the headway-sensitivity space for lane 1 (a) and lane 2 (b). The solid lines represent neutral stability curves and the dotted lines coexisting curves. ($v^1_{\max}=2.5$ m/s, $v^2_{\max}=2$ m/s, $h_{1c}=4.5$ m, and $h_{2c}=4$ m). For each set of $(\beta_1,\beta_2,\lambda_1)$ on lane 1 or $(\beta_1,\beta_2,\lambda_2)$ on lane 2, the space is divided into three regions by solid line and dotted line: stable region above the dotted line, metastable region between the solid line and the dotted line, and unstable region below solid line.

$$\tau_l = \frac{\beta_1 + 1.5\beta_2 + 2\lambda_l}{3V_l'(h_l)}. \tag{14}$$

For small disturbances with long wavelengths, the uniform traffic flow is unstable in the condition that

$$\tau_l > \frac{\beta_1 + 1.5\beta_2 + 2\lambda_l}{3V_l'(h_l)}. \tag{15}$$

The neutral stability curves in the parameter space $(\Delta x_l, \alpha_l)$ are shown in Fig. 1, where the sensitivity $\alpha_l = 1/\tau_l$. Obviously, there exist the critical points (h_{lc}, α_{lc}) for the neutral stability subject to different sets of $(\beta_1,\beta_2,\lambda_1)$ for lane 1 and $(\beta_1,\beta_2,\lambda_2)$ for lane 2. The apex of each curve indicates the critical point. On each lane, the uniform state irrespective

of weighted headway is always linearly stable for $\alpha_l > \alpha_{lc}$, while uniform states in a neighborhood h_{lc} are unstable for $\alpha_l < \alpha_{lc}$. The traffic flow is stable above the neutral stability curve and a traffic jam will not appear. While below the curve, traffic flow is unstable and the density waves emerge. From Fig. 1 it can be seen that with taking into account the lateral effects ($\beta_2 > 0$), the critical points and the neutral stability curves are lowered, which means the stability of the uniform traffic flow on each lane has been strengthened. The traffic jam is thus suppressed efficiently. Ge *et al.* [25] reported that in the case of single lane traffic, the traffic flow stability can be improved by considering more vehicles ahead in the car-following model; we here obtain the same result on flow stability improvement but by incorporating lateral effects in traffic modeling.

IV. NONLINEAR ANALYSIS

We now consider the slowly varying behaviors for long waves in the stable and unstable regions. Introduce slow scales for space variable n_l and time variable t [25], and define the slow variables X_l and T as follows:

$$X_l = \varepsilon(n_l + b_l t) \quad \text{and } T = \varepsilon^3 t, \quad 0 < \varepsilon \ll 1, \quad l = 1,2, \tag{16}$$

where b_l is a constant to be determined. Let

$$\Delta x_{l,n_l}(t) = h_{lc} + \varepsilon R_l(X_l, T). \tag{17}$$

Rewriting Eq. (6) in terms of the headways, yields

$$\begin{aligned}\Delta x_{l,n_l}(t + 2\tau_l) = {} & \Delta x_{l,n_l}(t + \tau_l) + \tau_l[V_l(\Delta x_{l,n_l+1}, \Delta_{l,n_l+1}) \\ & - V_l(\Delta x_{l,n_l}, \Delta_{l,n_l})] + \lambda_l \tau_l[\Delta x_{l,n_l+1}(t + \tau_l) \\ & - \Delta x_{l,n_l+1}(t) - \Delta x_{l,n_l}(t + \tau_l) + \Delta x_{l,n_l}(t)],\end{aligned} \tag{18}$$

where $V_l(\Delta x_{l,n_l}, \Delta_{l,n_l}) = V_l(\Delta \bar{x}_{l,n_l})$, $\Delta \bar{x}_{l,n_l} = \beta_1 \Delta x_{l,n_l} + \beta_2 \Delta_{l,n_l}$. Substituting Eqs. (16) and (17) into Eq. (18) and making the Taylor expressions to the fifth order of ε, we obtain the following nonlinear partial differential equation

$$\begin{aligned}& \varepsilon^2(b_l - V_l')\partial_{X_l} R_l + \varepsilon^3\left[\frac{3}{2}b_l^2\tau_l - \frac{V_l'}{2}(\beta_1 + 1.5\beta_2) - \lambda_l b_l\right]\partial_{X_l}^2 R_l \\ & + \varepsilon^4\left\{\partial_T R_l + \left[\frac{7b_l^3\tau_l^2}{6} - \frac{V_l'}{6}(\beta_1 + 2.5\beta_2) - \frac{3\lambda_l(1 + b_l\tau_l)b_l}{6}\right]\partial_{X_l}^3 R_l - \frac{V_l'''}{6}\partial_{X_l} R_l^3\right\} \\ & + \varepsilon^5\left\{3b_l\tau_l\partial_T\partial_{X_l} R_l + \left[\frac{5}{8}b_l^4\tau_l^3 - \frac{V_l'}{24}(\beta_1 + 7.5\beta_2)\right]\partial_{X_l}^4 R + \frac{V_l'''}{12}(\beta_1 + 1.5\beta_2)\partial_{X_l}^2 R_l^3\right\} \\ & + \lambda_l\varepsilon^5\left[\partial_{X_l}\partial_T R_l + \frac{4b_l^3\tau_l^2 + 6b_l^2\tau_l + 4b_l}{24}\partial_{X_l}^4 R_l + \frac{\lambda_l V_l'''}{6}\partial_{X_l}^2 R_l^3\right] = 0,\end{aligned} \tag{19}$$

where $V_l' = dV_l(\Delta \bar{x}_{l,n_l}) / d\Delta \bar{x}_{l,n_l}\big|_{\Delta \bar{x}_{l,n_l} = h_{lc}}$ and $V_l''' = d^3 V_l(\Delta \bar{x}_{l,n_l}) / d^3 \Delta \bar{x}_{l,n_l}\big|_{\Delta \bar{x}_{l,n_l} = h_{lc}}$. Near the critical point (h_{lc}, α_{lc}), taking $\tau_l = (1 + \varepsilon^2)\tau_{lc}$, $b_l = V_l'$ and $\tau_{lc} = (\beta_1 + 1.5\beta_2 + 2\lambda_l)/3V_l'$, then Eq. (19) can be simplified as

$$\begin{aligned}& \partial_T R_l + \left[\frac{7 - 8\lambda_l + 10\lambda_l^2 - 9\beta_1 - 22.5\beta_2}{54}\right]V_l'\partial_{X_l}^3 R_l - \frac{V_l'''}{6}\partial_{X_l} R_l^3 \\ & + \varepsilon\left[\left(\frac{A_{l0}}{2}\right)V_l'\partial_{X_l}^2 R_l + B_{l0}V_l'\partial_{X_l}^4 R_l + \frac{A_{l0}}{12}V_l'''\partial_{X_l}^2 R_l^3\right] = 0.\end{aligned} \tag{20}$$

where $A_{l0} = \beta_1 + 1.5\beta_2 + 2\lambda_l$ and $B_{l0} = [5A_{l0}^3 - 9(\beta_1 + 7.5\beta_2) + 4\lambda_l A_{l0}^2 + 18\lambda_l A_{l0} + 36\lambda_l]/216$. We make the following transformations for Eq. (20):

$$\begin{aligned}T' &= -\frac{7 - 8\lambda_l + 10\lambda_l^2 - 9\beta_1 - 22.5\beta_2}{54}T, \\ R_l &= \left[\frac{7 - 8\lambda_l + 10\lambda_l^2 - 9\beta_1 - 22.5\beta_2}{9V_l'''}V_l'\right]^{1/2}R_l'.\end{aligned} \tag{21}$$

Thus, we obtain the regularized equation

$$\begin{aligned}& \partial_{T'} R_l' - \partial_{X_l}^3 R_l' + \partial_{X_l} R_l'^3 \\ & + \varepsilon\left(\frac{27}{2}C_1^l\partial_{X_l}^2 R_l' - \frac{1}{2}C_2^l\partial_{X_l}^4 R_l' + \frac{1}{2}C_3^l\partial_{X_l}^2 R_l'^3\right) = 0,\end{aligned} \tag{22}$$

where $C_1^l = -2A_{l0}/D_{l0}$, $C_2^l = -[5A_{l0}^3 - 9(\beta_1 + 7.5\beta_2) + 4\lambda_l A_{l0}^2 + 18\lambda_l A_{l0} + 36\lambda_l]/2D_{l0}$, $C_3^l = A_{l0}$, $D_{l0} = 7 - 8\lambda_l + 10\lambda_l^2 - 9\beta_1 - 22.5\beta_2 \leqslant 0$, $0 \leqslant \lambda_l \leqslant 1$, $l = 1,2$.

Equation (22) is the modified KDV equation with an $o(\varepsilon)$ correction term. We first ignore the $o(\varepsilon)$ term and get the KDV equation with the kink-antikink soliton solution

$$R_{l,0}'(X_l, T') = \sqrt{c_l}\tanh\sqrt{\frac{c_l}{2}}(X_l - c_l T'), \quad l = 1,2, \tag{23}$$

where c_l is the propagation velocity of the kink-antikink soliton solution. In order to determine the selected value of propagation velocity c_l for the solution (23), the following solvability condition must be satisfied:

$$(R_{l,0}', M[R_{l,0}']) = \int_{-\infty}^{+\infty} dX_l\, R_{l,0}'(X_l, T')M[R_{l,0}'(X_l, T')] = 0, \tag{24}$$

where $M[R_{l,0}'] = 13.5C_1^l\partial_{X_l}^2 R_{l,0}' + 0.5C_2^l\partial_{X_l}^4 R_{l,0}' - 0.5C_3^l\partial_{X_l}^2 R_{l,0}'^3$. By performing the integration, we obtain the selected velocity c_l

$$c_l = \frac{135C_1^l}{2C_2^l + 3C_3^l}, \quad l = 1,2. \tag{25}$$

Hence, we obtain the kink-antikink soliton solution of the KDV equation (23), i.e.,

$$R_l(X_l,T)=\left[\frac{(7-8\lambda_l+10\lambda_l^2-9\beta_1-22.5\beta_2)}{9V_l'''}V_l'c_l\right]^{1/2}\times\tanh\sqrt{\frac{c_l}{2}}\left(X_l+\frac{7-8\lambda_l+10\lambda_l^2-9\beta_1-22.5\beta_2}{54}V_l'c_lT\right),\quad l=1,2. \tag{26}$$

If the optimal velocity function takes the form of Eq. (7), then $V_1'=1$, $V_1'''=-2$, $V_2'=5/4$, $V_2'''=-5/2$. The amplitude A_i of the kink solution is given by

$$A_l=\left[-\frac{7-8\lambda_l+10\lambda_l^2-9\beta_1-22.5\beta_2}{18}c_l\left(\frac{\alpha_{lc}}{\alpha_l}-1\right)\right]^{1/2}, \tag{27}$$

where $\alpha_{lc}=\tau_{lc}=3V_l'/(\beta_1+1.5\beta_2+2\lambda_l)$. The kink solution represents the coexisting phase which consists of the freely moving phase with low density and the jammed phase with high density. The headways of freely moving phase and jammed phase are given by $\Delta x_l=h_{lc}-A_l$ and $\Delta x_l=h_{lc}+A_l$, respectively. According to these, we can depict all coexisting curves in the $(\Delta x_l,\alpha_l)$ plane, as shown by dotted lines in Fig. 1.

In Fig. 1, for each set of $(\beta_1,\beta_2,\lambda_1)$ on lane 1 or $(\beta_1,\beta_2,\lambda_2)$ on lane 2, the traffic flow is divided into three regions by the solid line (representing the neutral stability curve) and the dotted line (representing the coexisting curve): the first is the stable region above the coexisting curve, the second is the metastable region between the neutral stability curve and the coexisting curve, and the third is the unstable region below the neutral stability curve. We can see that both the stability and coexisting curves decrease with the increasing values of β_2 and λ_l, $l=1,2$. Hence, the stability region is enlarged, and the metastable, and unstable regions are reduced.

V. SIMULATION RESULTS

In the Xue's single lane model [21], it was shown that the triangular shock wave, soliton wave and kink wave appear in three regions—stable, metastable and unstable regions, respectively. In our two-lane model incorporating the lateral effects in traffic, these three waves appear too, respectively described by the solutions of the Bergers' equation, KDV equation and MKDV equation constructed in the three regions, respectively. In this section, we numerically describe the kink-antikink density wave as a traffic jam in the unstable region and discuss the space-time evolution of the headways on lane 1 and lane 2 with respect to different sets of $(\beta_1,\beta_2,\lambda_l)$. The simulation is based on Eq. (18) for headways. Suppose that there N_l vehicles distributed on lane l under a periodic boundary condition. The initial headways for both lanes are given below: $\Delta x_{1,n_1}(t)|_{t=0,1}=5.0$ for $n_1\neq 0.5N_1$ and $n_1\neq 0.5N_1+1$, $\Delta x_{1,n_1}(t)|_{t=0,1}=5.0-0.1$ for $n_1=0.5N_1$, $\Delta x_{1,n_1}(t)|_{t=0,1}=5.0+0.1$ for $n_1=0.5N_1+1$; $\Delta x_{2,n_2}(t)|_{t=0,1}=4.0$ for $n_2\neq 0.5N_2$ and $n_2\neq 0.5N_2+1$, $\Delta x_{2,n_2}(t)|_{t=0,1}=4.0-0.1$ for $n_2=0.5N_2$, $\Delta x_{2,n_2}(t)|_{t=0,1}=4.0+0.1$ for $n_2=0.5N_2+1$. The total number of vehicles is $N_1=160$ for lane 1 and $N_2=200$ for lane 2. The safety distance is $h_{1c}=4.5$ m for lane 1 and $h_{1c}=4.0$ m for lane 2. The initial values of the lateral distances Δ_{1,n_1} and Δ_{2,n_2} can be calculated according to the initial positions of all vehicles on both lanes. Other input parameters for the simulation are $v_{\max}^1=2.5$ m/s, $v_{\max}^2=2$ m/s, $\alpha_1=2.5$, and $\alpha_2=2$.

Figure 2 shows the space-time evolution of the headways on lane 1 and lane 2 for different sets of $(\beta_1,\beta_2,\lambda_1,\lambda_2)$. In patterns (a), (b), and (c), the traffic flow is unstable because the instability condition (16) is satisfied. When small disturbances are added to the uniform traffic flows on both lanes in (a), (b), and (c), they are amplified with time and the uniform flows on both lanes change finally to inhomogeneous traffic flows; the traffic jam in (a) is more serious than that in (b), that in (b) more serious than that in (c); the disturbances in (d) disappear and the traffic flows on both lanes become uniform over the whole space. The patterns (b) and (c) show that only considering relative velocity or only considering lateral effects is not enough to eliminate disturbances. Patterns (a) and (b) verify that in the unstable region, the kink-antikink soliton solution indeed appears as traffic jams. In addition, in (a), (b), and (c), the density waves propagate backwards.

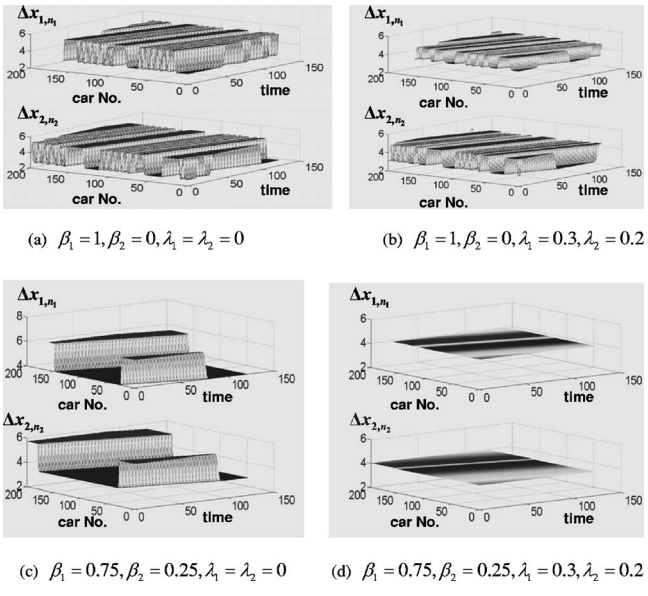

FIG. 2. Space-time evolution of the headways on lane 1 and lane 2 after $t=10\,000$ s. The patterns (a),(b),(c) are for the coexisting phases, and (d) for the freely moving phase. (The numbers 0, 50, 100, and 150 on time axis represent 10 000, 10 050, 10 100, and 10 150, respectively.)

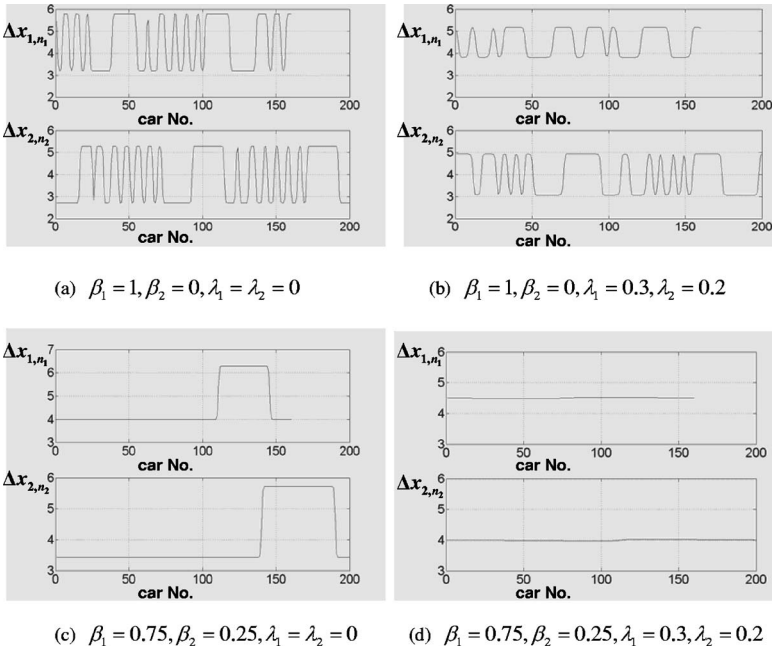

FIG. 3. Headways profile of the density waves at $t=10\,120$. In (a), (b), and (c), the kink-antikink waves appear, and in (d) the kink density wave disappears.

Figure 3 shows the headway profiles at sufficiently large time $t=10\,120$ s. With the same sensitivity parameters ($\alpha_1=2.5$, $\alpha_2=2$), as the relative velocity and further the lateral effects are considered, the amplitude of the density wave decreases. In pattern (d) the density waves disappear and the traffic flows on both lanes are uniform over the whole space. All the above results show that the consideration of lateral effects could stabilize traffic flow. The simulation outcomes are in agreement with analytical results.

VI. SUMMARY

We have extended the OV car-following model of single lane to the case with two lanes through taking into account the lateral effects. The traffic nature has been analytically analyzed by using the linear and nonlinear analyses. It has been shown that there exists critical point in the extended model and the neutral stability line is obtained. Obviously, the consideration of lateral effects could stabilize the traffic flows on both lanes. The MKDV equation has been derived to describe the traffic behavior near the critical point. We gave simulation results to show the analytical analyses clearly. The simulation outcomes about the space-time evolution of the headways on both lanes are in good agreement with analytical results. The lane changing actions do not truly occur and are not explicitly formulated in the proposed model but only worried about by drivers. Even though, our study shows that this anxiousness indeed has influence upon people's driving behavior and could stabilize traffic flow.

ACKNOWLEDGMENTS

This work was supported by the National Natural Science Foundation of China.

[1] D. Chowdhury, L. Santen, and A. Schreckenberg, Phys. Rep. **329**, 199 (2000).
[2] M. Bando, K. Hasebe, A. Nakayama, A. Shibata, and Y. Sugiyama, Phys. Rev. E **51**, 1035 (1995).
[3] M. Bando, K. Hasebe, K. Nakanishi, and A. Nakayama, Phys. Rev. E **58**, 5429 (1998).
[4] L. C. Davis, Phys. Rev. E **66**, 038101 (2002).
[5] I. Lubashevsky, P. Wagner, and R. Mahkne, Eur. Phys. J. B **32**, 243 (2003).
[6] T. Komatsu and S. I. Sasa, Phys. Rev. E **52**, 5574 (1995).
[7] T. Nagatani and K. Nakanishi, Phys. Rev. E **57**, 6415 (1998).
[8] M. Muramatsu and T. Nagatani, Phys. Rev. E **60**, 180 (1999).
[9] T. Nagatani, Phys. Rev. E **60**, 6395 (1999).
[10] D. Helbing and B. Tilch, Phys. Rev. E **58**, 133 (1998).
[11] M. Treiber, A. Hennecke, and D. Helbing, Phys. Rev. E **59**, 239 (1999).
[12] I. Lubashevsky, P. Wagner, and R. Mahnke, Phys. Rev. E **68**, 056109 (2003).
[13] W. Helly, in *Proceedings of the Symposium on Theory of Traffic Flow*, edited by R. C. Herman (Elsevier, New York, 1959), p. 207.
[14] M. Treiber and D. Helbing, cond-mat/9901239 (unpublished).
[15] M. Treiber, A. Hennecke, and D. Helbing, Phys. Rev. E **62**, 1805 (2000).
[16] R. Jiang, Q. Wu, and Z. Zhu, Phys. Rev. E **64**, 017101 (2001).
[17] R. Jiang, Q. S. Wu, and Z. J. Zhu, Transp. Res., Part B: Methodol. **36**, 405 (2002).
[18] Y. Xue, L. Y. Dong, Y. W. Yuan, and S. Q. Dai, Commun. Theor. Phys. **38**, 230 (2002).
[19] Y. Xue, L. Y. Dong, Y. W. Yuan, and S. Q. Dai, Acta Phys. Sin.

51, 492 (2002).
[20] Y. Xue, Chin. Phys. **11**, 1128 (2002).
[21] Y. Xue, Acta Phys. Sin. **53**, 25 (2004).
[22] H. Lenz, C. K. Wagner, and R. Sollacher, Eur. Phys. J. B **7**, 331 (1998).
[23] K. Hasebe, A. Nakayama, and Y. Sugiyama, Phys. Rev. E **69**, 017103 (2004).
[24] K. Hasebe, A. Nakayama, and Y. Sugiyama, Phys. Rev. E **68**, 026102 (2003).
[25] H. X. Ge, S. Q. Dai, L. Y. Dong, and Y. Xue, Phys. Rev. E **70**, 066134 (2004).
[26] G. Orosz, R. E. Wilson, and B. Krauskopf, Phys. Rev. E **70**, 026207 (2004).